

Supplementary Material to “External Prior Guided Internal Prior Learning for Real Noisy Image Denoising”

Anonymous CVPR submission

Paper ID 1047

In this supplementary material, we provide:

1. The closed-form solution of the proposed weighted sparse coding model in the main paper.
2. More denoising results on the real noisy images (with no “ground truth”) provided in the dataset [1].
3. More denoising results on the 15 cropped real noisy images (with “ground truth”) used in the dataset [2].
4. More denoising results on the 60 cropped real noisy images (with “ground truth”) from [2].

1. Closed-Form Solution of the Weighted Sparse Coding Problem (4)

The weighted sparse coding problem in the main paper is:

$$\min_{\alpha} \|\mathbf{y} - \mathbf{D}\alpha\|_2^2 + \|\mathbf{w}^T \alpha\|_1. \quad (1)$$

Since \mathbf{D} is an orthonormal matrix, problem (1) is equivalent to

$$\min_{\alpha} \|\mathbf{D}^T \mathbf{y} - \alpha\|_2^2 + \|\mathbf{w}^T \alpha\|_1. \quad (2)$$

For simplicity, we denote $\mathbf{z} = \mathbf{D}^T \mathbf{y}$. Since $\mathbf{w}_i = c * 2\sqrt{2}\sigma^2 / (\Lambda_i + \varepsilon)$ is positive (please refer to Eq. (18) in the main paper), problem (2) can be written as

$$\min_{\alpha} \sum_{i=1}^{p^2} ((\mathbf{z}_i - \alpha_i)^2 + \mathbf{w}_i |\alpha_i|). \quad (3)$$

The problem (3) is separable w.r.t. α_i and can be simplified to p^2 scalar minimization problems

$$\min_{\alpha_i} (\mathbf{z}_i - \alpha_i)^2 + \mathbf{w}_i |\alpha_i|, \quad (4)$$

where $i = 1, \dots, p^2$. Taking derivative of α_i in problem (4) and setting the derivative to be zero. There are two cases for the solution.

(a) If $\alpha_i \geq 0$, we have

$$2(\alpha_i - \mathbf{z}_i) + \mathbf{w}_i = 0. \quad (5)$$

The solution is

$$\hat{\alpha}_i = \mathbf{z}_i - \frac{\mathbf{w}_i}{2} \geq 0. \quad (6)$$

So $\mathbf{z}_i \geq \frac{\mathbf{w}_i}{2} > 0$, and the solution $\hat{\alpha}_i$ can be written as

$$\hat{\alpha}_i = \text{sgn}(\mathbf{z}_i) * (|\mathbf{z}_i| - \frac{\mathbf{w}_i}{2}), \quad (7)$$

where $\text{sgn}(\bullet)$ is the sign function.

(b) If $\alpha_i < 0$, we have

$$2(\alpha_i - \mathbf{z}_i) - \mathbf{w}_i = 0. \quad (8)$$

The solution is

$$\hat{\alpha}_i = \mathbf{z}_i + \frac{\mathbf{w}_i}{2} < 0. \quad (9)$$

So $\mathbf{z}_i < -\frac{\mathbf{w}_i}{2} < 0$, and the solution $\hat{\alpha}_i$ can be written as

$$\hat{\alpha}_i = \text{sgn}(\mathbf{z}_i) * (-\mathbf{z}_i - \frac{\mathbf{w}_i}{2}) = \text{sgn}(\mathbf{z}_i) * (|\mathbf{z}_i| - \frac{\mathbf{w}_i}{2}). \quad (10)$$

In summary, we have the final solution of the weighted sparse coding problem (1) as

$$\hat{\alpha} = \text{sgn}(\mathbf{D}^T \mathbf{y}) \odot \max(|\mathbf{D}^T \mathbf{y}| - \mathbf{w}/2, 0), \quad (11)$$

where \odot means element-wise multiplication and $|\mathbf{D}^T \mathbf{y}|$ is the absolute value of each entry of the vector $\mathbf{D}^T \mathbf{y}$.

2. More Results on Dataset [1]

In this section, we give more visual comparisons of the competing methods on the real noisy images provided in [1]. As can be seen from Fig. 1-4, our proposed method performs better than the state-of-the-art denoising methods. This validates the effectiveness of our proposed external prior guided internal prior learning framework for real noisy image denoising.

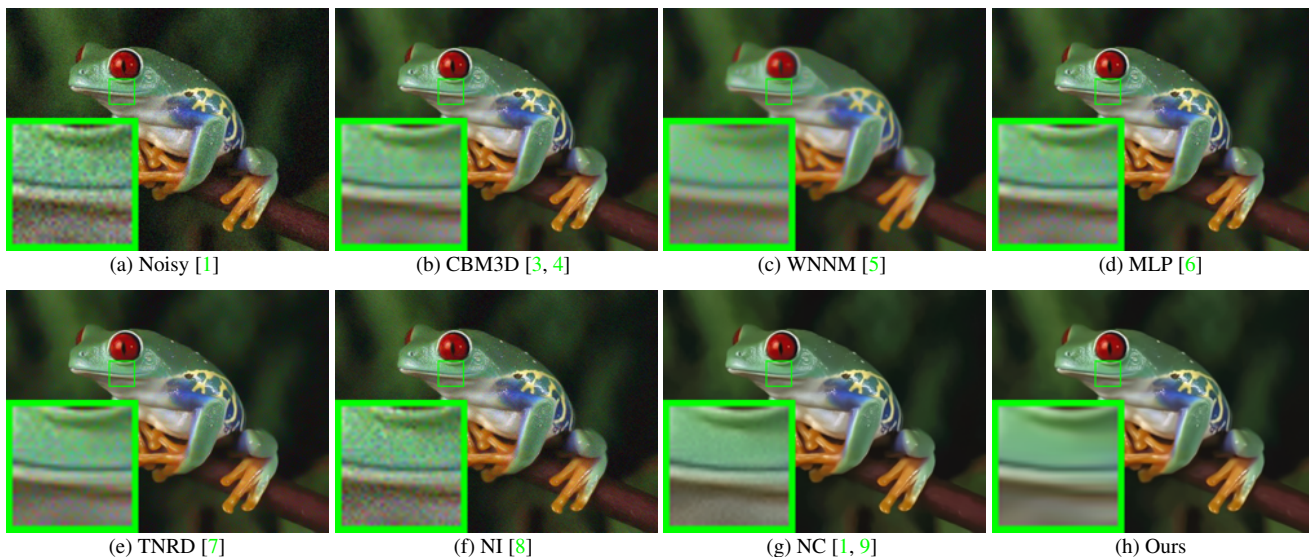


Figure 1. Denoised images of the real noisy image “Frog” [1] by different methods. The images are better to be zoomed in on screen.

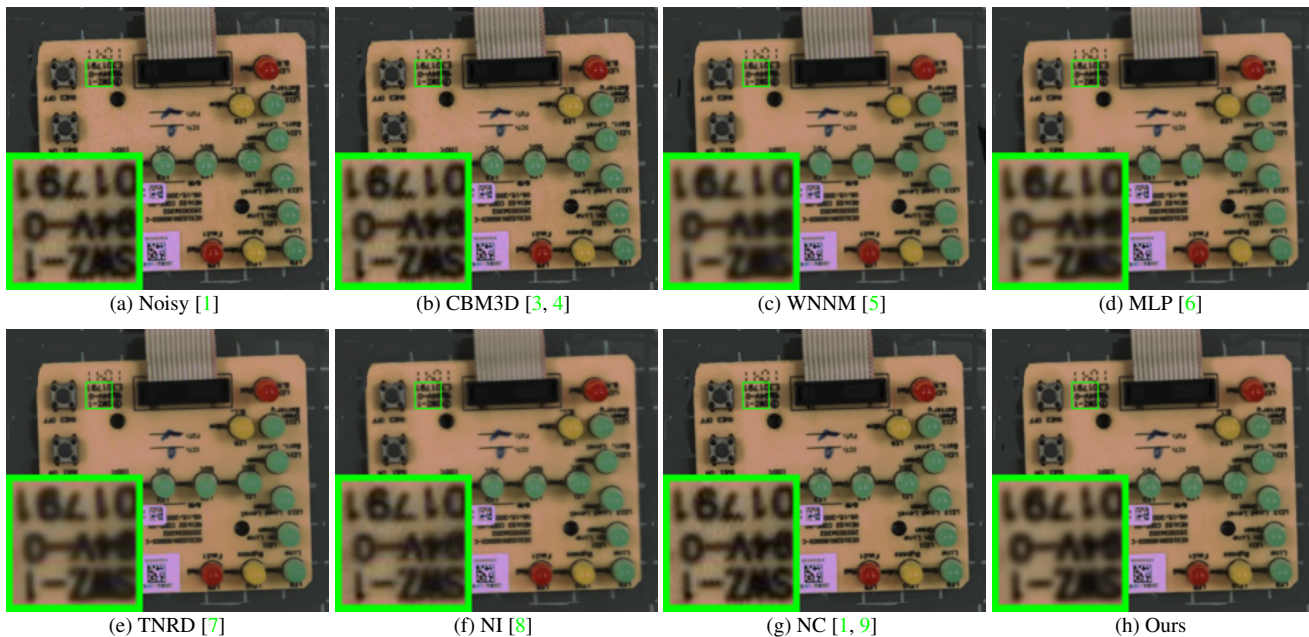


Figure 2. Denoised images of the real noisy image “Circuit” [1] by different methods. The images are better to be zoomed in on screen.

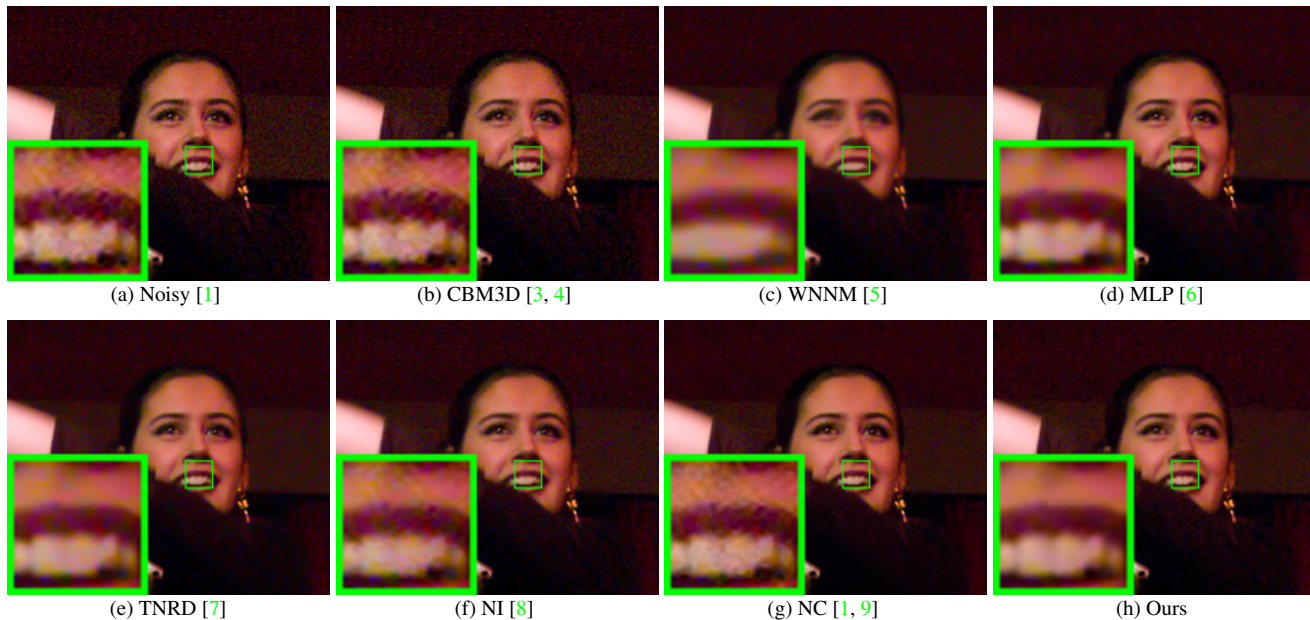


Figure 3. Denoised images of the real noisy image “Woman” [1] by different methods. The images are better to be zoomed in on screen.

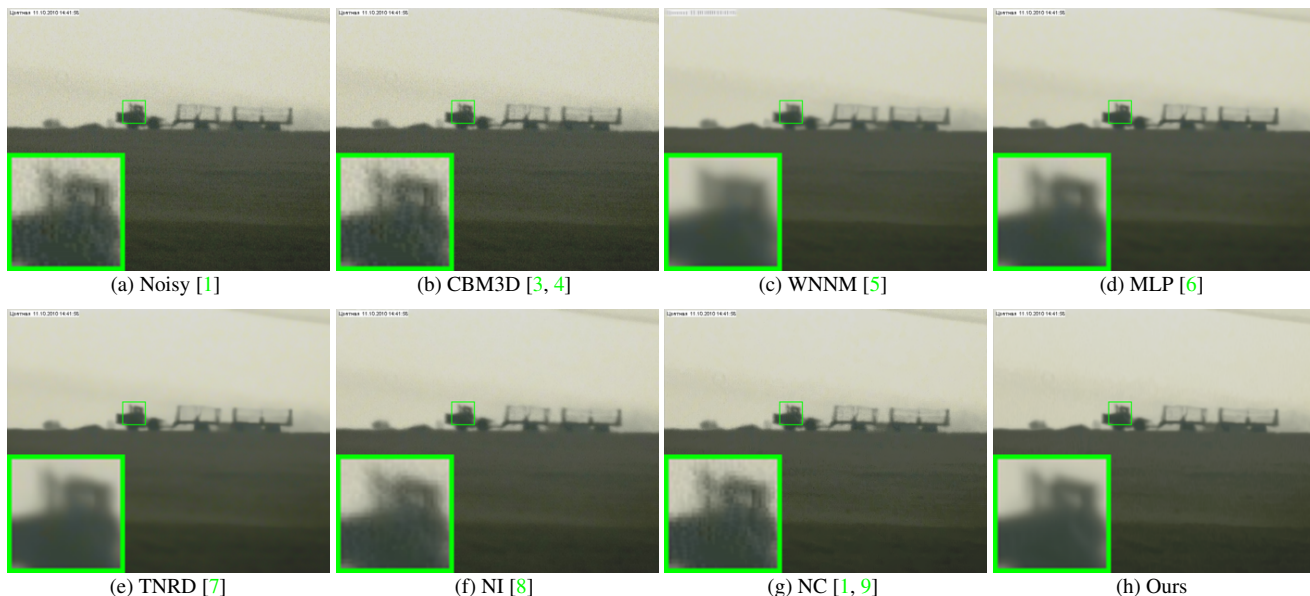


Figure 4. Denoised images of the real noisy image “Vehicle” [1] by different methods. The images are better to be zoomed in on screen.

References

- [1] M. Lebrun, M. Colom, and J. M. Morel. The noise clinic: a blind image denoising algorithm. <http://www.ipol.im/pub/art/2015/125/>. Accessed 01 28, 2015. 1, 2, 3
- [2] S. Nam, Y. Hwang, Y. Matsushita, and S. J. Kim. A holistic approach to cross-channel image noise modeling and its application to image denoising. *IEEE Conference on Computer Vision and Pattern Recognition (CVPR)*, pages 1683–1691, 2016. 1
- [3] K. Dabov, A. Foi, V. Katkovnik, and K. Egiazarian. Image denoising by sparse 3-D transform-domain collaborative filtering. *IEEE Transactions on Image Processing*, 16(8):2080–2095, 2007. 2, 3

324			378
325	[4]	K. Dabov, A. Foi, V. Katkovnik, and K. Egiazarian. Color image denoising via sparse 3D collaborative filtering with grouping constraint in luminance-chrominance space. <i>IEEE International Conference on Image Processing (ICIP)</i> , pages 313–316, 2007. 2, 3	379
326			380
327	[5]	S. Gu, L. Zhang, W. Zuo, and X. Feng. Weighted nuclear norm minimization with application to image denoising. <i>IEEE Conference on Computer Vision and Pattern Recognition (CVPR)</i> , pages 2862–2869, 2014. 2, 3	381
328			382
329	[6]	H. C. Burger, C. J. Schuler, and S. Harmeling. Image denoising: Can plain neural networks compete with BM3D? <i>IEEE Conference on Computer Vision and Pattern Recognition (CVPR)</i> , pages 2392–2399, 2012. 2, 3	383
330			384
331	[7]	Y. Chen, W. Yu, and T. Pock. On learning optimized reaction diffusion processes for effective image restoration. <i>IEEE Conference on Computer Vision and Pattern Recognition (CVPR)</i> , pages 5261–5269, 2015. 2, 3	385
332			386
333	[8]	Neatlab ABSOft. Neat Image. https://ni.neatvideo.com/home . 2, 3	387
334			388
335	[9]	M. Lebrun, M. Colom, and J.-M. Morel. Multiscale image blind denoising. <i>IEEE Transactions on Image Processing</i> , 24(10):3149–3161, 2015. 2, 3	389
336			390
337			391
338			392
339			393
340			394
341			395
342			396
343			397
344			398
345			399
346			400
347			401
348			402
349			403
350			404
351			405
352			406
353			407
354			408
355			409
356			410
357			411
358			412
359			413
360			414
361			415
362			416
363			417
364			418
365			419
366			420
367			421
368			422
369			423
370			424
371			425
372			426
373			427
374			428
375			429
376			430
377			431